Methanol sorption and permeability in Nafion and acid-doped PBI and ABPBI membranes

Liliana A. Diaz [a,b], Graciela C. Abuin [b], Horacio R. Corti [a,*]

[a] Departamento de Física de Materia Condensada, Centro Atómico Constituyentes, Comisión Nacional de Energía Atómica (CNEA), B1650KNA San Martín, Buenos Aires, Argentina
[b] Instituto Nacional de Tecnologia Industrial (INTI), B1650KNA San Martín, Buenos Aires, Argentina

ARTICLE INFO

ABSTRACT

Methanol permeability in phosphoric acid-doped membranes based in poly[2,2′-(m-phenylene)-5,5′-bibenzimidazole] (PBI) and poly[2,5-benzimidazole] (ABPBI), prepared by two different casting procedures, were measured using a diffusion cell in the temperature range from 20 to 90 °C, along with the electrical conductivity at 30 and 60 °C. The permeability results, the first reported for ABPBI membranes, were compared to commercial Nafion 117 and commercial crosslinked ABPBI and correlated with differences in water and methanol sorption behavior of these materials, determined using a quartz crystal microbalance (QCM) on ultra-thin films (<100 nm). Methanol partition constant was calculated from ^{1}H NMR analysis of the membrane desorption products in heavy water. The performance of ABPBI as methanol barrier is poorer than PBI, but it is more than one order of magnitude less permeable to methanol than Nafion® 117 all over the temperature range. The commercial ABPBI membrane has slightly lower permeability than the ABPBI membrane obtained by high-temperature casting, indicating that an optimized casting procedure could be more efficient than crosslinking to reduce methanol crossover. The combination of low methanol uptake, high proton conductivity and, mainly, low methanol permeability make ABPBI membranes attractive as proton exchange membranes in direct methanol fuel cells.

© 2012 Elsevier B.V. All rights reserved.

1. Introduction

Nafion, a perfluorosulfonated ionomer, is commonly used as electrolyte membrane in direct methanol proton exchange membrane fuel cells (DMPEM), but a number of alternative ionomeric materials are being tested to overcome its main disadvantages: dehydration that occurs at temperatures higher than 100 °C and methanol crossover problem associated with the high permeability of methanol through Nafion, that significantly lowers the electrochemical efficiency of DMPEM fuel cells [1].

Thus, membranes based on PBI (poly-2,2′-p-(phenylene)-5,5′-bibenzimidazole), PBI modified structures such as ABPBI (poly(2,5)-benzimidazole), whose structures are shown in Fig. 1, composites of PBI with inorganic compounds, and blends with Nafion or other polymers, are being evaluated as candidates for PEM and DMPEM fuel cells [2–8]. Polybenzimidazole based membranes are neutral, but become acceptable proton conductors when doped with acids, mainly with H_3PO_4. The interest in the development of this kind of membranes for high temperature PEM fuel cells is based on its high oxidative and thermal stability [9], while their use in DMPEM fuel cells relies on their low methanol crossover [2].

Hydrogen production by methanol electrolysis (methanol electrochemical reforming) is also a field of potential interest for these membranes [10–12].

Although there is an extensive literature related to polybenzimidazole materials, it is necessary to study more deeply methanol permeability in different types of polybenzimidazole membranes for application to DMPEM fuel cells, such as PBI and ABPBI, prepared by different methods and compare results with that obtained in commercial membranes, such as Nafion. Proton conductivity to methanol permeability ratio determines the membrane selectivity [6], which is a parameter related to the performance of the membrane in DMFC.

The permeability of vapor water, hydrogen and oxygen in several kind of undoped and doped PBI membranes have been studied by several authors [13–15], including a microporous PBI membrane used for gas separation [16,17], and N-substituted PBI membranes. The permeability of several gases, including hydrogen and oxygen has been recently reported for undoped N-substituted ABPBI [18].

A review of the properties of PBI membranes by Li et al. [2] summarizes most of methanol permeability studies in PBI and modified PBI. Two methods of studying methanol permeability or crossover through the membranes have been described. The first method determines the methanol crossover from anode to cathode in an operating DMPEM fuel cell by measuring the steady-state current near the open-circuit voltage (OCV) and determining the
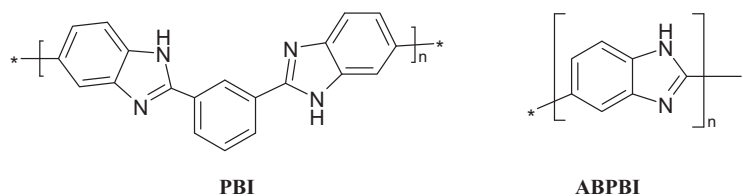
Fig. 1. Structure of PBI and ABPBI polymers.

flow of CO_2 at the cathode outlet, assuming complete conversion of methanol into CO_2 [19]. The second method use the traditional two-chamber diffusion cell to measure the methanol flow through the membrane, from the donor reservoir at constant methanol concentration, to the receptor reservoir initially containing water [4].

The main purpose of this work is to study the methanol permeability of ABPBI membranes prepared by casting using different procedures and compare the results with those obtained for commercial crosslinked ABPBI and Nafion membranes, and membranes prepared with commercial PBI.

The inclusion of Nafion 117 membranes in this study has two purposes. Firstly, to validate the permeation procedure we have adopted, and secondly to obtain reliable values for the methanol permeability in this membrane, due to the large scatter observed in the results reported in the literature. Thus, methanol permeation in Nafion could be compared with that in acid-doped PBI and ABPBI membranes on a more rigorous basis.

Several authors have studied the permeability of methanol through PBI [4,19–26], fluorinated PBI [27,28], and PBI blends with other polymers [6,8,29–31], as can be seen in Table 1. Methanol permeability through acid-doped PBI depends on the H_3PO_4 doping level, defined as the moles of acid per imidazole ring (λ_a), as well on the methanol concentration and temperature. Table 1 clearly indicated that these three basic parameters were not controlled in most of the previous studies, and the comparison of the results is troublesome owing to temperature or acid doping level differences, measured as H_3PO_4 moles per mole of repetitive polymer unit (λ'_a). For this reason we included PBI in this study, in order to compare its permeability with that of ABPBI under similar conditions.

It is worth to note that PBI permeability results in two chambers diffusion cell were performed mainly at ambient temperature, except for the works by Pu et al. [20,21] who measured liquid methanol permeability up to 50 °C, and that by Wainright et al. [25], who reported vapor methanol permeability above 100 °C.

As far as we know there is no methanol permeability data reported for the ABPBI membranes. Therefore, this study provides the first data of methanol permeability on ABPBI membranes obtained by two different casting procedures, based on polymer synthesized in our laboratory. Also, we report here methanol permeability through a commercial crosslinked ABPBI membrane. In addition, the partition coefficients of methanol between the aqueous solution and the membranes were determined, which allowed us to calculate the diffusion coefficient of methanol through the membranes. Finally, we studied the electrical conductivity of all the membranes to demonstrate that improving methanol permeability in ABPBI membranes is not tied to a depletion of their capacity to transport protons.

2. Experimental

2.1. Membrane preparation

ABPBI was prepared by condensation of 3,4-diaminobenzoic acid (DABA) monomer in polyphosphoric acid (PPA) following the procedure reported by Gómez Romero et al. [32]
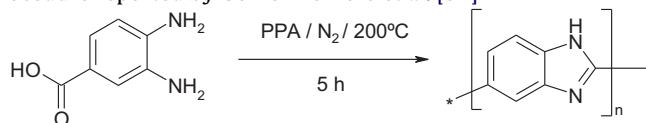
3,4-diaminobenzoic acid   ABPBI

The resulting polymer was condensed in water, dried at 90 °C, grinded, and washed with water. Then it was washed with aqueous NaOH (10%, w/w) during 20 h in order to eliminate remaining polyphosphoric acid, washed with water until neutral pH, and finally it was dried at 90 °C.

High temperature casting ABPBI membranes (ABPBI-HT) were prepared by heating on a glass plate at about 70 °C a 5 wt% ABPBI solution in methanesulfonic acid. After a few hours the solvent was eliminated and the plate was immersed in water to separate the membrane. Low temperature ABPBI membranes (ABPBI-LT) were casted from a solution of 4.2 wt% ABPBI and 2.7 wt% NaOH in ethanol on a Teflon plate, cooled with vapor from a liquid N_2 vessel in order to obtain a low evaporation rate. Ethanol was evaporated overnight in a ventilated hood and the membrane could be easily separated from the plate.

PBI membranes were prepared by casting from a 5 wt% solution of PBI powder (Goodfellow) in dimethylacetamide (DMAc) in a vacuum furnace at 80 °C during 4 h.

All casted PBI and ABPBI membranes, having thickness between 50 and 150 μm, were doped in 10.64 M H_3PO_4 for 72 h in order to protonate the imidazole ring. The same doping procedure was used with the commercial crosslinked ABPBI membranes Fumapem A (Fumatech).

Table 1
Summary of methanol permeation studies in PBI and PBI composite membranes.

Polymer	Method	Conditions	T (°C)	Ref.
PBI	TCDC[a]	λ'_a = 4.5; c_{CH3OH}: not reported	Ambient	[4]
PBI	OCV[b]	λ'_a = 5; c_{CH3OH}: 0.25–1.00 mole fraction	180	[19]
PBI	TCDC	λ'_a = 1.8; c_{CH3OH}: 10–100 wt%	25–50	[20,21]
PBI	TCDC	λ_a = 0 ; c_{CH3OH}: 1 M	NI	[22]
PBI	TCDC	λ'_a = ?; c_{CH3OH}: 20–100 wt%	NI	[23]
PBI	FCV[c]	λ'_a = 6.7; c_{CH3OH}: 1–14 M	125–200	[24]
PBI	TCDC	λ'_a = 5; vapor (93.3 kPa)	120–192	25]
PBI	OCV	λ'_a = ?; c_{CH3OH}: 0.5–4 M	60–90	[26]
FPBI	TCDC	λ'_a = 3 ; c_{CH3OH}: 6 wt%	Ambient	[27]
FPBI	TCDC	λ'_a = 0, 1.2, 3.0; c_{CH3OH}: 6 wt%	Ambient	[28]
PBI/Nafion	TCDC	PBI: 4–8%; c_{CH3OH}: 1 M	60	[6]
PBI/Nafion	TCDC	Thin films of PBI on Nafion	NI	[8]
PBI/Nafion	OCV	Thin films of PBI on Nafion; c_{CH3OH}: 10 wt%	NI	[30]
PBI/SPOP	TCDC	PBI: 0–12 wt%; c_{CH3OH}: 1 M	60	[29]
PBI/SPEEK	TCDC	PBI: 5–20%	NI	[31]

[a] Two compartment diffusion cell.
[b] Open circuit voltage in direct methanol fuel cell;.
[c] Fuel cell voltammetry.

Table 2
Doping degree (λ_a) and free acid content (λ_f) at 25 °C for PBI and ABPBI membranes doped in 10.64 M aqueous H_3PO_4.

Membrane	λ_a	λ_f
ABPBI-LT	2.5	0.095
ABPBI-HT	2.8	0.093
	2.9[a]	
ABPBI-C	1.5	0.03
PBI	1.9	0.095
	2.5[a]	
	2.0[b]	

[a] Ref. [34].
[b] Ref. [23].

Commercial Nafion 117® (Ion-Power) membranes were cleaned in H_2O_2 3 wt%, at 80 °C, during 1 h and rinsed one hour in boiling water. Then, they were immersed one hour in 1 M H_2SO_4, at 80 °C, and finally rinsed again in boiling during one more hour.

Thicknesses of membrane samples used in the methanol permeability experiments were measured by means of a Mahr XL1-57B-15 dead load gauge.

N,N-dimethilacetamide (Merck), H_3PO_4 (Merck), H_2O_2 (Merck), H_2SO_4 (Baker Analyzed), 3,4-diaminobenzoic acid, 97% (Aldrich), polyphosphoric acid 85% (Aldrich), methanesulfonic acid 99.5+% (Aldrich) and methanol (J.T. Baker) all analytical grade were used as received. Water was deionized and passed through a Millipore filter.

2.2. Properties of the PBI and ABPBI polymers

The molecular weight of PBI and ABPBI polymers, and phosphoric acid uptake of PBI and ABPBI-HT membranes has been reported elsewhere, together with the properties of an ABPBI membrane casted at low temperature from formic acid [33]. We briefly summarize here the main results.

The molecular weight of ABPBI was determined from viscosity measurements of its solutions in concentrated 96 wt% H_2SO_4 using a Cannon – Fenske 150 viscosimeter. The value of the extrapolated intrinsic viscosity at 30 °C was 2.35 dl g^{-1} for ABPBI and, resorting to the Mark–Houwink equation [34], the averaged molecular weight of the polymer was $M_p = 18,800$. For PBI, the extrapolated intrinsic viscosity at 30 °C was 0.482 dl g^{-1}, and molecular weight, $M_p = 19,600$.

Phosphoric acid uptake of ABPBI-LT ethanol casted membranes was measured employing the method described in [33]. The phosphoric acid uptake and the free acid content of the ABPBI-HT, ABPBI-LT, and PBI polymers, measured in terms of acid moles per imidazole ring [33], are summarized in Table 2.

2.3. Water and methanol uptake

A quartz crystal microbalance (QMB) was used to measure the water–methanol uptake of the membranes from the vapor phase. Thin membrane films, in the range of 100 nm in thickness, were prepared by direct casting on the quartz crystal. This method allows a rapid sorption equilibration as compared to bulky membranes. Typically, it takes few minutes to reach a stationary weight of the film on the QMB, compared to several hours or few days, which are necessary in the conventional gravimetric method for thick membranes.

The QMB was placed within a chamber and a stream of dry nitrogen was circulated through it in order to obtain the mass of the dry film. Afterwards dry nitrogen was replaced by a stream of nitrogen previously bubbled through a methanol aqueous solution in the range of methanol concentration 0–100 wt%. The concentration of methanol in the vapor phase can be calculated from the

composition of the aqueous solution by means of the liquid/vapor equilibrium curves for methanol–water mixtures at 0.1 MPa [35]. As expected, the methanol molar fraction in the vapor is higher than in the liquid, but along this work we will use the molar fraction of methanol in the liquid phase (x_{CH3OH}) as a measure of the composition in order to facilitate the comparison of membrane solvent sorption from the liquid phase. This choice is supported by the fact that the driven force for sorption is the difference in chemical potential between the external media and the membrane, and the isopiestic guarantee that the chemical potential in the liquid and in the vapor phase are the same under the experimental conditions.

The mass change of membranes equilibrated with methanol–water mixtures was determined from the measurement of the resonant frequency shift by means of the Sauerbreyıs equation [36].

The methanol/water uptake of membranes at 20 °C can be expressed as λ, the ratio between the total moles of water plus methanol ($n_{H2O} + n_{CH3OH}$) sorbed per mol of sulphonic groups ($M_p = 1100$ g mol^{-1}) for Nafion membranes, or per mol of monomer unit containing one imidazol ring in the case of PBI ($M_p = 142$ g mol^{-1}) or ABPBI ($M_p = 116$ g mol^{-1}) membranes,

$$\lambda = \frac{(n_{H2O} + n_{CH3OH})M_p}{m_p} \tag{1}$$

where m_p is the mass of dry polymer. Alternatively, the methanol/water uptake can be expressed as mass of water plus methanol sorbed, $m_s = m_{H2O} + m_{CH3OH}$, by gram of dry polymer, m_s/m_p.

The water–methanol uptake of the membranes from the liquid phase at the methanol concentration used in the permeability experiments (20 wt%, or methanol molar fraction $x_{CH3OH} = 0.12$) was also determined. The membrane sample was immersed in a closed vessel containing the methanol solution during several days. Once the equilibration was reached the sample was removed from the solution, dried superficially with tissue paper, and immersed in a small vial containing a known mass (around 2 g.) of D_2O (99.97 wt%) under N_2 flow to avoid degradation of the heavy water. After several days water and methanol originally sorbed in the membrane pass to the heavy water phase, and a known mass of sodium acetate is added to the solution. The determination of water and methanol in the solution was performed through the measure of the ^1H NMR spectra using a Bruker Avance II 500 NMR spectrometer at 500.13 MHz with full ^{13}C decoupling. The integrated areas of methanol and water peaks were compared to that of the sodium acetate used as a reference.

From the known masses of methanol and water in the membrane, and the composition of the equilibration solution, the partition constant of methanol between both phases, K, can be calculated as:

$$K = \frac{m*_{CH3OH}(m_{CH3OH} + m_{H2O})}{m_{CH3OH}(m*_{CH3OH} + m*_{H2O})} \tag{2}$$

where m_i and m^*_i are the mass of species i in the solution and in the membrane, respectively. That is, K is the ratio of the methanol mass fraction in the membrane and the solution, taking the mass fraction of methanol in the membrane on the water/methanol basis.

2.4. Methanol permeability

Methanol permeability through the membranes was measured using a stainless steel two-chamber diffusion cell (TCDC), shown in Fig. 2. The volumes of the compartments are 11.3 cm^3 each, and the membrane sample was clamped between the compartments by means of two PTFE ring frames, exposing a membrane permeation area of 3.14 cm^2. The membrane was sandwiched with two
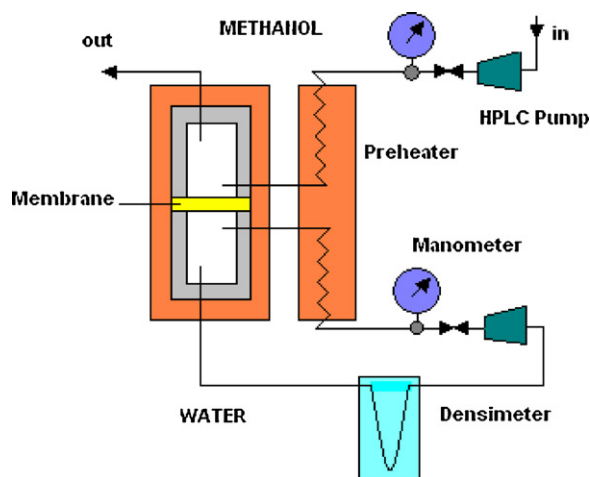
Fig. 2. Scheme of two-chamber permeation equipment showing the open methanol donor loop (upper part) and the closed methanol receptor loop (bottom part).

Fig. 3. Methanol concentrations profiles in the donor and receptor compartments and inside the membrane (linear gradient assumed).

stainless steel meshes in order to avoid its deformation due to uneven pressures on both chambers during the experiments.

As indicated in Fig. 2, the permeation cell was connected to the fluid circulation system, comprising two HPLC piston pumps (Gilson 305 Master pump) and a preheater chamber for setting the fluid temperature slightly lower than the working temperature. A proportional temperature controller was used to fix the temperature of the permeation cell, which was measured using a Platinum Thermoresistor. Tubing was made of PEEK (poly-ether-ether-ketone) in cold parts and stainless steel in hot parts.

One compartment was filled with aqueous 20 wt% methanol solution (donor) and the other with pure water (receptor) in the case of permeability measurements in Nafion and undoped PBI membranes. In order to keep a constant methanol concentration at the donor side, the aqueous methanol solution was recirculated at a flow rate of 1 cm^3 min^{-1} and the solution was discarded once it passed through the cell. Pure water, also at a flow rate of 1 cm^3 min^{-1}, was circulated for several minutes through the receptor side and discarded to allow the stationary methanol concentration gradient be formed across the membrane. Then, the water loop was closed ($t=0$) through an 'on line' vibrating tube densimeter (VTD), immersed in a bath at 25 °C, which was used to determine the methanol concentration as a function of time in the receptor compartment. The total closed loop circulating volume was measured after each experiment and varied between 17 cm^3 and 18 cm^3.

Methanol permeability measurements in doped PBI and ABPBI membranes were carried out using the same experimental procedure, except that a 20 wt% methanol/10.64 M H$_3$PO$_4$ was circulated across the donor compartment, and 10.64 M H$_3$PO$_4$ was recirculated across the receptor compartment, in order to keep constant the acid uptake of the acid-doped PBI and ABPBI membranes. This is an important difference with previous TCDC studies (Table 1) because in those works the acid-doped membranes were in contact with water and aqueous methanol solutions of quite different water activities, which could lead to changes in the water content inside the membrane.

During the permeation experiment the methanol concentration in the receptor compartment loop was monitored with the VTD, previously calibrated with methanol aqueous solutions in the range 0–7 wt% of methanol in water or in 10.64 M H$_3$PO$_4$ aqueous solutions. Typically the methanol concentration in the receptor compartment loop was allowed to rise up to about 1 wt% methanol in order to maintain the methanol concentration gradient across the membrane almost unperturbed.
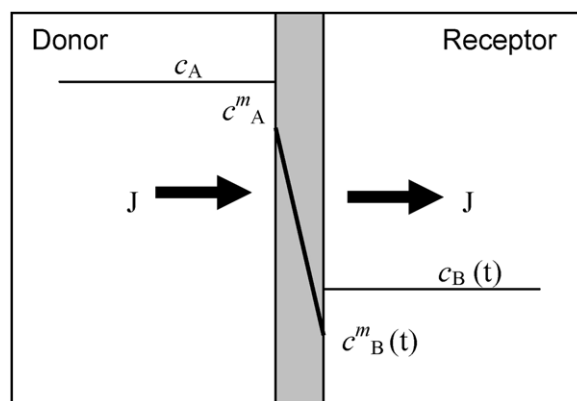
Thus, the flux, J (moles of methanol per unit area and unit time) of methanol through the membrane can be expressed using the well-known Fick-like equation:

$$J = P \left(\frac{\partial c_s}{\partial x} \right) \tag{3}$$

where P is the permeability coefficient of methanol in the membrane, and the subfix s means that the methanol concentration gradient is measured in the solution side (see Fig. 3). The relationship between the permeability coefficient and the diffusion coefficient, D, is obtained when the partition constant $K = c_m/c_s$, relating the ratio of concentrations in the solution, c_s, and in the membrane, c_m, is considered. Thus,

$$P = DK \tag{4}$$

and the determination of D from the measured methanol flux through the membrane requires the knowledge of the partition constant of methanol between the aqueous and membrane phases.

Methanol concentration (measured in mol dm^{-3}) in the donor compartment was held at a constant value (c_A), and the methanol concentration in the receptor compartment as a function of time, $c_B(t)$, was measured. According to Eq. (3), if a linear methanol concentration gradient is assumed inside the membrane,

$$\frac{dc_B(t)}{dt} = \frac{AP}{V_B L} [c_A - c_B(t)] \tag{5}$$

where V_B is the total closed loop volume of the receptor side, A is the measuring membrane exposed area, and L is the membrane thickness. Eq. (5) can be integrated, yielding,

$$\ln \left(1 - \frac{c_B(t)}{c_A} \right) = -\frac{AP}{V_B L} t \tag{6}$$

This expression is simpler than that obtained when the methanol concentration in the donor compartment is not constant [37] and it facilitates the data treatment. Fig. 4 shows the results of methanol permeation for an ABPBI-LT membrane, where the stationary state is reached after approximately 20 min and the permeability coefficient is obtained from the linear part of the curve.

In the case $c_B(t) \ll c_A$, the linear expression is recovered from Eq. (6),

$$\frac{c_B(t)}{c_A} = \frac{AP}{V_B L} t \tag{7}$$

This condition is fulfilled in our experiments because the maximum methanol concentration in the receptor compartment never exceeded $c_B(t) = 0.05 c_A$.
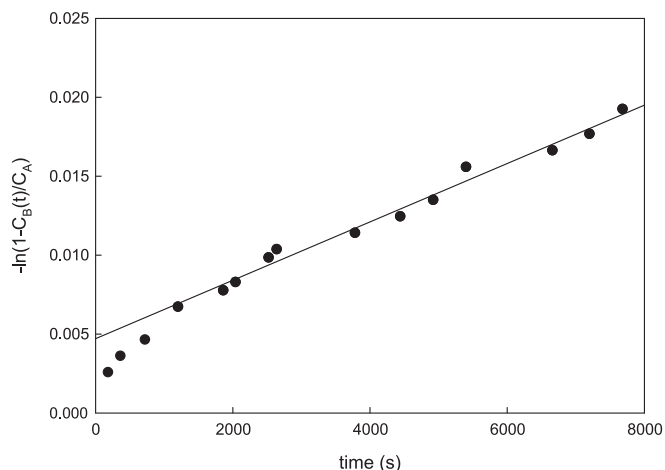
Fig. 4. Typical methanol permeation plot for a ABPBI-LT membrane at 26 °C with $c_A = 7.58$ M. The permeation coefficient was obtained from Eq. (6) from the linear part of the curve.

2.5. Electrical conductivity

For the electrical conductivity measurements the membranes were cut in strips (1 cm width and 3 cm length) and equilibrated in liquid water before the measurements, performed using a 4-electrode cell. The cell has holes to allow the membrane to be exposed to water vapor when enclosed in a glass vessel containing water and thermostatized at 30 and 60 °C.

The impedance of the samples was measured using an Auto-Lab PGSTAT 302 N with impedance analyzer module (FRA), in the frequency range 50 Hz–100 kHz with a current of 10 μA. The resistance of the membrane was obtained from the Nyquist diagram. The specific conductivity of the membrane was calculated from the measured resistance, R, using the equation:

$$\sigma = \frac{l}{R \cdot \delta \cdot b} \tag{8}$$

where l is the distance between electrodes, δ the membrane thickness and b the membrane width.

3. Results and discussion

3.1. Water–methanol uptake and partition constant

Fig. 5a shows the sorption of water/methanol from the vapor phase as a function of the solution composition for Nafion, PBI and ABPBI-LT, expressed as mass of solvent per gram of dry membrane (m_s/m_p). These results obtained from ultra-thin films through the QCM method, should be taken cautiously because the sorption in ultra-thin films could be different from that obtained in thick membranes. However, the comparison clearly indicates that the sorption of water–methanol by doped PBI and ABPBI membranes is much higher than for Nafion, when expressed as m_s/m_p. Water/methanol sorption does not change appreciably with the solution compositions for PBI and ABPBI, as indicate by the linear fit shown in Fig. 5a. Solvent sorption in Nafion clearly increases with the methanol content of the solution and it is approximately double for methanol in relation to water.

In Fig. 5b the same results are expressed in terms of λ (Eq. (1)), and the behavior of the Nafion uptake is different than that observed for PBI and ABPBI. Polybenzimidazols sorbs less methanol than water and the sorption dependence on the solution composition are monotonous. Expressed as moles of solvent per mole of ionic groups, the sorption in Nafion of pure water ($\lambda_w = 6.26$) and pure methanol ($\lambda_m = 6.34$) are very similar, indicating that Nafion
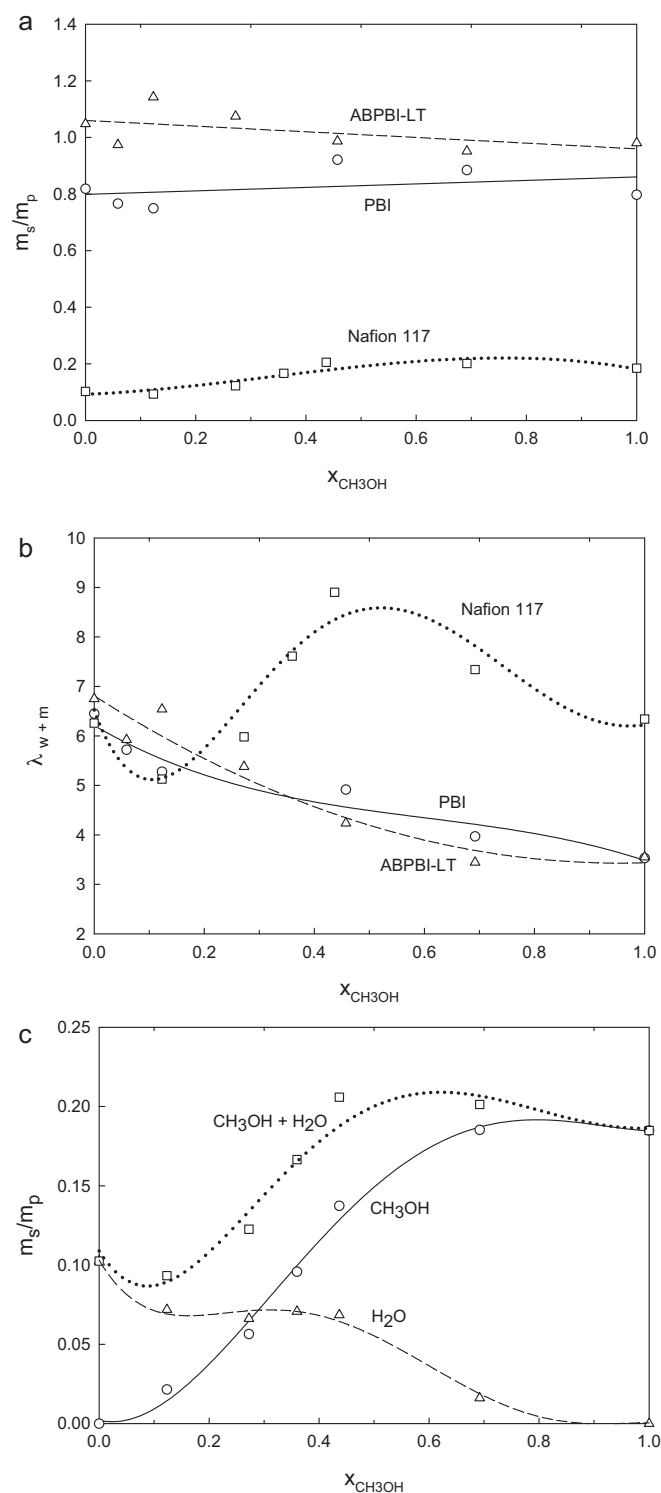

Fig. 5. Water–methanol sorption of ultra-thin membranes at room temperature as a function of the composition: (a) Nafion 117 (27 nm), PBI (100 nm), and ABPBI-LT (76 nm), expressed as m_s/m_p; (b) the same as in (a) expressed as λ; (c) sorption of water and methanol in Nafion, expressed as m_s/m_p (see text for details). Lines in (b) and (c) are just a help for eyes.

does not exhibit preferential sorption by any of these solvents. On the contrary, pure water sorption in PBI and ABPBI almost doubles pure methanol sorption as expressed in terms of λ_w and λ_m, that is, these membranes have a clear preference for the sorption of water over methanol.

Table 3
Water and methanol uptake at 25 °C by Nafion, PBI, and ABPBI membranes.

Membrane	Methanol wt%	x_{CH3OH}	λ_w	λ_m	K
Nafion	20	0.12	13.5 ± 1.9	3.95 ± 0.25	1.15 ± 0.07
PBI	20	0.12	3.48 ± 0.10	0.63 ± 0.02	1.23 ± 0.05
ABPBI-C	20	0.12	3.15 ± 0.62	0.31 ± 0.07	0.75 ± 0.01
ABPBI-HT	20	0.12	5.83	0.72	1.00
	50	0.36	2.11	1.05	0.94
	75	0.63	0.79	1.34	1.00

Table 4
Methanol permeation rate, permeability and diffusion coefficient in Nafion 117 membranes as a function of temperature.

T (°C)	c_A (wt%)	P (10^6 cm^2 s^{-1})	D^a (10^6 cm^2 s^{-1})
20	20	$0.69 \pm 0,10$	0.60 ± 0.09
30	10	0.69 ± 0.05	
	20	0.79 ± 0.05	0.69 ± 0.05
	40	0.57 ± 0.09	
60	20	1.78 ± 0.20	
90	20	5.31 ± 0.03	

[a] Calculated with an average partition constant $K = 1.15$ in the range 20–30 °C.

The water/methanol sorption behavior of Nafion as a function of composition is complex. It decreases when methanol is added to water and with further methanol addition increases reaching a maximum at a methanol molar fraction close to 0.5 (where it sorbs almost 50% more liquid mixtures compare to the pure solvents). In Fig. 5c the sorption of water and methanol in Nafion, expressed as m_s/m_p, are plotted as a function of the composition. Values of λ_w and λ_m were calculated using the total λ and the partition constant of methanol in Nafion. It is observed that the water uptake is relatively constant up to $x_{CH3OH} \approx 0.45$, and decrease sharply to cero for $x_{CH3OH} > 0.45$, while the methanol uptake increase monotonously up to $x_{CH3OH} \approx 0.6$ and remain constant in the methanol-rich region. This behavior is slightly different to that recently reported by Chaabane et al. [38] for Nafion 117, where it was observed that λ_w is also constant in the water rich region, but λ_m and λ_w increase monotonously with the methanol content in the solution. Taking into account that our results correspond to ultra-thin Nafion films, where the effect of the substrate on the solvent uptake could be important, the qualitative agreement with the sorption results in Nafion 117 is remarkable.

Results of water and methanol sorption from liquid methanol aqueous solutions (20 wt%) in thick membranes are summarized in Table 3 for Nafion 117, PBI, commercial ABPBI, and ABPBI-HT membranes. The water sorption, expressed as λ_w, follows the trend observed for ultra-thin membranes, except for Nafion, which exhibits a sorption much higher than that found in ultrathin membranes. This fact has been confirmed by a systematic study we have performed on the water sorption on ultra-thin Nafion membranes on different types of substrates [39], and it is related to the effect of the substrate on the microstructure of the membrane.

The sorption of water/methanol in ABPBI-HT membranes was measured at higher concentration of methanol (up to 75 wt%) and, as it can be seen in Table 3. The behavior is similar to that found in Fig. 5b for ABPBI-LT, that is, a monotonous decreases of λ with increasing methanol molar fraction in the solution.

The water sorption by the commercial crosslinked ABPBI membrane is lower than that of the ABPBI-HT membrane, and similar to that of the PBI. Also, the sorption of methanol by the crosslinked membrane is lower than those by PBI and ABPBI-HT. Thus, the effect of crosslinking in ABPBI is to reduce the swelling by water to levels similar to that found in PBI and, at the same time, it seems to increase the selectivity toward water compared to methanol.

Methanol partition constants, K, calculated according to Eq. (2), and reported in Table 3, indicate that Nafion and PBI membranes are slightly enriched in methanol ($K > 1$), while ABPBI-HT membranes has not selectivity towards water or methanol ($K \approx 1$) all over the range of composition studied (20–75 wt%). The commercial crosslinked ABPBI membrane seems to sorbs water selectively ($K < 1$), as mentioned above. Our results for methanol partition constant in Nafion confirm those already reported by other authors [38,40], while those for PBI and ABPBI are the first reported in the literature for these membranes. Thus, diffusion coefficients of methanol in the membranes could be calculated from the measured permeability coefficients, at temperatures close to 25 °C.

3.2. Methanol permeability in Nafion 117

Nafion 117 is the PEM more studied in the literature and its methanol permeability has been reported by several groups in relation to its performance in DMPEM fuel cells, taking into account the effect of membrane pretreatment on the solute permeation [37,41–52].

Table 4 shows the methanol permeability through Nafion® 117 (thickness 178 μm) from a 20 wt% methanol aqueous solution as a function of temperature in the range from 20 °C to 90 °C. The effect of the methanol concentration is also illustrated in the measurements at 30 °C, where a slight maximum in permeability is observed for a methanol solution around 20 wt%. Diffusion coefficients calculated using Eq. (4) are also reported in Table 4 at 20 and 30 °C.

Methanol permeability in Nafion is shown in Fig. 6, along with those determined by several authors using different methods and membrane pretreatments. A typical Nafion membrane conditioning involves the hydration of the commercial membrane in boiling 3% H_2O_2 solution, followed by boiling in demineralized water and 0.5 M H_2SO_4. This is the procedure adopted in this work and also by Ren et al. [44], Zhou et al. [46], Every et al. [47], and Wu et al. [49,50]. On the other hand, some authors hydrated the commercial membrane at room temperature [41,43,52] or dried the membrane under vacuum before hydration [42,43,49], preheat the membrane above 100 °C [42,51] or use the membrane without any treatment [45,48]. Most of the permeability measurements were performed using a diffusion method similar to that described here, except Ren et al. [44], who obtained the methanol permeation through the
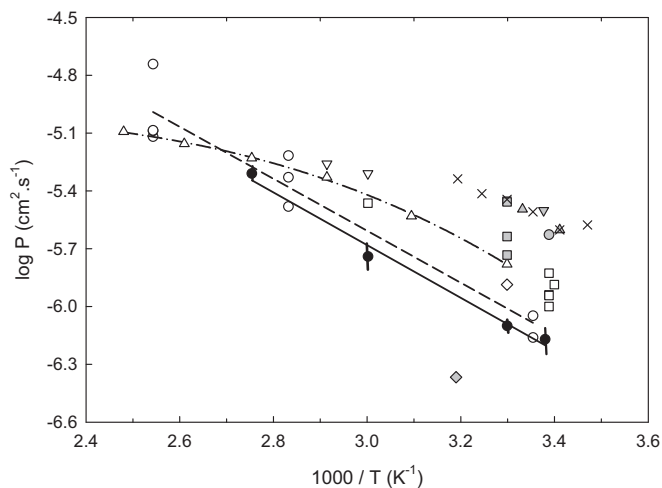

Fig. 6. Temperature dependence of the methanol permeability coefficient in Nafion 117 membranes: (●) this work; (▽) [41]; (□) [42,43]; (△) [44]; (◆) [45]; (○) [46]; (◇) [47]; (▼) [48]; (●) [49]; (▲) [37,50]; (■) [51]; (×) [52]. The solid, dashed and dot-dashed curves are the best fit for the data from this study, Refs. [46,44], respectively.
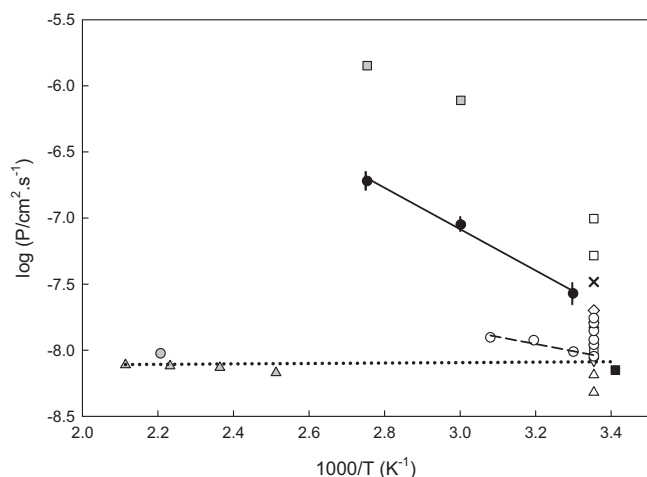
Fig. 7. Temperature dependence of the methanol permeability of PBI membranes: this work ($\bullet$)(doped); ($\blacksquare$)(undoped); ($\triangledown$)[22]; ($\lozenge$)[4]; ($\square$)[28]; ($\triangle$)[23]; ($\bigcirc$)[20,21]; ($\times$)[27]; ($\blacksquare$)[26]; ($\bullet$)[19]; ($\blacktriangle$)[24].

Nafion membrane by measuring the current for electro-oxidation of methanol in a fuel cell.

It is clear that the dispersion of the data is large when the whole set of data is analyzed. Thus, at room temperature the permeability coefficients spread over more than one order of magnitude. The dispersion is lower when only the membranes treated in boiling aqueous H_2O_2, water and aqueous H_2SO_4 are compared. Thus, our permeability results are slightly lower than those reported by Zhou et al. [46] up to 120 °C. The activation energy of the methanol permeation process can be calculated from the Arrhenius plot and the calculated value is 25.3 kJ mol^{-1}, in very good agreement to the activation energy obtained by Zhou et al. (25.8 kJ mol^{-1}) [46]. Ren et al. [44] reported values of activation energy close to 20 kJ mol^{-1}, although it is evident in Fig. 4 that their results do not obey Arrhenius equation.

The data by Tricoli et al. [42,43] at room temperature clearly show the effect of different membrane treatment on the permeability results. As received membranes seem to exhibit a lower permeability [51,52], except for the case of the study by Feichtinger et al. [45].

We conclude that our results, along with those reported over a similar range of temperatures [44,46] yield permeability values, which agree reasonable well taking into account differences in the measurement technique and methanol concentration.

3.3. Methanol permeability in undoped and doped PBI

As mentioned above, several authors studied the permeability of methanol through PBI membranes under different experimental conditions [4,19–26]. It is well known that PBI is a better methanol barrier than Nafion, but the results summarized in Fig. 7, indicate that the methanol permeability at room temperature for PBI spread over more than one order of magnitude. The scatter of data is probably due to the different acid doping conditions and methanol concentration used in the experiments.

Our results, summarized in Table 5, were obtained for PBI membranes with $\lambda_a = 1.9$ and methanol concentration 20 wt% in the donor chamber. Also the permeability of an undoped PBI membrane was determined at 20 °C, and the results agree with those reported by Pivovar et al. [22], confirming that methanol permeability through undoped PBI membrane is lower than in doped ones. It is also noted that the PBI membranes with $\lambda_a = 0.9$ studied by Pu et al. [20,21] exhibit lower methanol permeability than our membranes. Also the results by Chuang et al. [28] at three different

Table 5
Methanol permeation rate, permeability and diffusion coefficient in PBI membranes as a function of temperature (methanol concentration: 20 wt%).

T (°C)	P (10^8 cm^2 s^{-1})	D^a (10^8 cm^2 s^{-1})
20 (undoped)	0.70 ± 0.06	
30 (doped)	2.68 ± 0.52	2.20 ± 0.45
60 (doped)	8.99 ± 0.93	
90 (doped)	19.1 ± 2.9	

^{a} Calculated with an average partition constant $K = 1.22$.

doping degrees (0, 0.6, and 1.5) show the same tendency, that is, the permeability to methanol increases with the doping level. This result is expected in view of the higher swelling and water content of the membranes associated to high acid contents.

The permeability data shown in gray in Fig. 7 were calculated from the CV methanol crossover current [19,24,26] assuming that six electron are involved in the cathodic methanol oxidation. In the case of the data by Lobato et al. [24] we assumed a membrane thickness of 30 μm [23]. A large scatter is observed for these data. Thus, the permeability reported by Gubler et al. [26] in the interval 60–90 °C is much higher than that measured at temperatures above 100 °C [19,24]. Curiously, the permeability coefficients at high temperatures are similar to that determined at ambient temperatures in undoped membranes, probably due to the fact that at high temperatures water and methanol desorbs from the membranes.

3.4. Methanol permeability in doped ABPBI: comparison with Nafion and PBI

As previously indicated, there are not reported data of methanol permeability and diffusion coefficients of ABPBI membranes. Our results for doped membranes prepared by high-temperature and low-temperature casting are shown in Table 6, along with the data for the commercial crosslinked ABPBI membrane.

A comparison of the methanol permeability of all the ABPBI membranes tested in this work is illustrated in Fig. 8. Permeability of ABPBI-HT is much lower than that of ABPBI-LT, which is consistent with the lower water content of the former [33]. It is interesting to note that the permeability data of the crosslinked ABPBI membrane as a function of temperature lies in between the permeability of both linear polymers.

For comparison, the methanol permeability data for PBI and Nafion membranes are also shown in Fig. 8. It is observed that methanol crossover current of methanol in PBI membranes is very
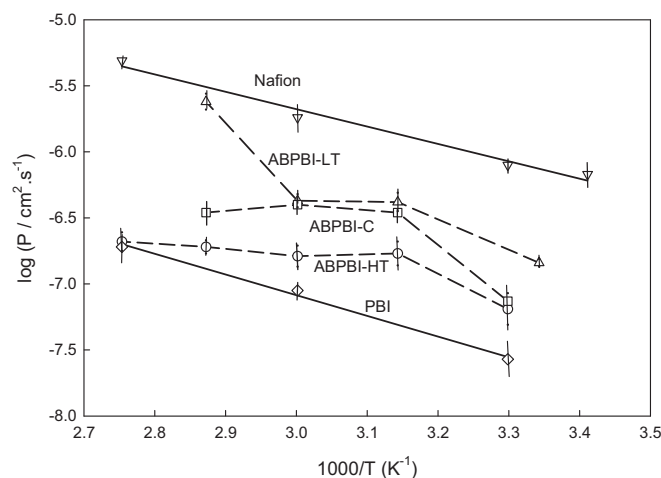

Fig. 8. Temperature dependence of the methanol permeability of doped ABPBI, doped PBI and Nafion membranes, methanol concentration 20% w/w. ($\bigcirc$) ABPBI-HT; ($\triangle$) ABPBI-LT; ($\square$) ABPBI-C; ($\lozenge$) PBI;($\triangledown$) Nafion 117.

Table 6
Methanol permeability and diffusion coefficient in ABPBI membranes, methanol concentration 20% w/w.

T (°C)	$P_{ABPBI-HT}$ (10^7 cm² s⁻¹)	$D_{ABPBI-HT}$[a] (10^7 cm² s⁻¹)	$P_{ABPBI-LT}$ (10^7 cm² s⁻¹)	$P_{ABPBI-C}$ (10^7 cm² s⁻¹)	$D_{ABPBI-C}$[b] (10^7 cm² s⁻¹)
26			1.46 ± 0.10		
30	0.65 ± 0.03	0.65 ± 0.04		0.735 ± 0.155	0.98 ± 0.22
45	1.68 ± 0.40		4.15 ± 0.69	3.45 ± 0.49	
60	1.63 ± 0.31		4.23 ± 0.50	3.95 ± 0.50	
75	1.90 ± 0.21		23.8 ± 3.4	3.43 ± 0.70	
90	2.07 ± 0.37				

[a] Calculated with $K = 1.00$.
[b] Calculated with $K = 0.75$.

small, contrary to that found in Nafion, in good agreement with previous results [1]. It was suggested that water uptake of the membrane largely determines the methanol permeation through the polymer [53], an assumption that could explain the results obtained in this work if we consider that λ is the sorption parameter which determines the methanol crossover. Pivovar et al. [54] have compared the swelling, methanol permeability and electro-osmotic drag of Nafion and undoped PBI and concluded that the large drag coefficients in Nafion is due to its relatively large, regular water-filled domains, as compared to the smaller ones in undoped PBI. Obviously, this explanation cannot be simply extrapolated to doped PBI, where the amount of water forming domains would be comparable to that in Nafion.

According to Pivovar et al. [54], the electro-osmotic drag could be a measure of the relative importance of the vehicle and Grotthuss mechanism of proton conduction. For proton conduction by Grotthuss mechanism one would not expect electro-osmotic drag. Then, the higher methanol crossover in Nafion compared to PBI and ABPBI could be explained by considering that the Grotthuss mechanism is predominant in PBI and ABPBI, while the vehicle mechanism is more important in Nafion. However, a recent study of the proton diffusion in Nafion 117 by electrical conductivity and NMR [55], indicates that only at low water uptake the vehicle mechanism is operating, while at high water uptake the proton conduction is mainly via Grotthuss mechanism. In consequence, the crossover of methanol in Nafion, PBI and ABPBI membranes at high hydration, as that usually found in normal DMPEM fuel cells operation, should be determined by normal permeation of methanol through the membrane driven by the concentration gradient.

Methanol permeation is determined by two factors: solubility (uptake) of methanol in the membrane and diffusion of the methanol inside the membrane. Our results indicate that the methanol uptake by PBI and ABPBI-HT membranes are similar, and approximately a factor 5 lower than the methanol uptake by Nafion, if thick membranes are compared (Table 3).

Although differences in methanol uptake are responsible, in part, for the higher methanol permeation through Nafion membranes as compared to PBI and ABPBI, differences in methanol permeability coefficients (and diffusion coefficients) between these membranes are very large. For instance, at 30 °C, the methanol permeability coefficient of Nafion is 50 times higher than that of PBI and between 8 and 17 times higher than the ABPBI membranes.

A possible explanation, according to Pu et al. [20], is that the barrier effect of PBI and ABPBI is influenced by the hydrogen bonds between methanol molecules and imidazole groups in the polymer. On the other hand, the higher permeability of doped PBI as compared to undoped PBI could be due to the presence of phosphoric acid molecules blocking or reducing the accessibility of methanol molecules to imidazole sites.

Finally, it should be noted that, as shown in Fig. 8, methanol permeation in doped PBI and Nafion increases with increasing temperature following the Arrhenius law. The calculated apparent activation energy for PBI, 30.1 kJ mol⁻¹, is greater than that reported by Pu et al. [20] for less doped PBI over a narrower range of temperature, and lower than the calculated from the data by Gubler et al. [26] in the interval 60–90 °C. The Arrhenius plot for ABPBI-HT leads to an averaged activation energy of 15.5 kJ·mol⁻¹ but, as can be observed in Fig. 8, the increase of permeability with temperature is much pronounced at low temperature and becomes very small at high temperature, in such a way that the permeability coefficient for ABPBI-HT is very close to that of PBI at 90 °C. The same trend is observed for ABPBI-C, although the methanol permeability is higher than that of PBI and ABPBI-HT. In summary, PBI and ABPBI-HT membranes are better barriers for methanol than Nafion all over the range of temperature studied, while ABPBI-HT membranes would exhibit better permeation properties than PBI beyond 90 °C.

3.5. Electrical conductivity of acid doped PBI and ABPBI

The specific conductivity of all the membranes studied in this work, at 30 and 60 °C, are summarized in Table 7. Except for ABPBI-C all the measured were performed with the membranes equilibrated with pure water vapor ($a_w = 1$).

Our results for PBI membranes agree quite well with those reported by Li et al. [56] and Hasiotis et al [57] at lower water activity. It seems that the water activity effect compensates the lower acid content in our PBI membrane. The conductivities of Nafion 117 membranes reported in Table 7 are higher than those previously reported [58] under identical conditions, probably as a consequence of different pretreatment of the membranes, and more than one order of magnitude higher than the conductivities of the PBI membranes.

Table 7
Specific conductivity of Nafion, PBI and ABPBI membranes at 30 and 60 °C.

Membrane	a_w	λ_a	κ (S cm⁻¹)/30 °C	κ (S cm⁻¹)/60 °C	Ref.
ABPBI-HT	1.00	2.8	0.0191 ± 0.0047	0.0410 ± 0.063	This work
ABPBI-LT	1.00	2.5	0.0085 ± 0.0012	0.0137 ± 0.0019	This work
ABPBI-C	0.33	–	0.0057 ± 0.0002	0.0034 ± 0.0004	This work
PBI	1.00	1.9	0.0061 ± 0.0007	0.0100 ± 0.0018	This work
	0.80–0.85	4.5	0.0054	0.0105	56
	0.80	5.0	0.003 (25 °C)	–	57
Nafion 117	1.00		0.092 ± 0.006	0.189 ± 0.013	This work
	1.00		0.068	0.140	58

Among the ABPBI membranes, the ABPBI-HT membrane exhibits the higher conductivity, more than twice the conductivity of the ABPBI-LT membrane, much higher than that of the commercial crosslinked ABPBI, although a factor 5 less conductive than the Nafion membrane. In spite of that the proton conductivity of the ABPBI membranes is compatible with their use in PEM fuel cells.

If a high value of the ratio between the proton conductivity and methanol permeability coefficient could be used as an indicator for a good membrane for direct methanol fuel cells [22] this ratio, calculated at $30\,^{\circ}$C, is 7×10^4 for Nafion, 8×10^4 for PBI, and 29×10^4 for ABPBI-HT (units: S. cm^{-3}), which clearly indicate that the ABPBI membrane prepared by the high temperature casting procedure described in this work would be an excellent candidate for this type of fuel cells.

4. Conclusions

Methanol permeability through Nafion and phosphoric acid-doped PBI and ABPBI membranes were measured using a two-chamber diffusion cell in the temperature range from 20 to $90\,^{\circ}$C. The ABPBI membranes, which can be suitable for application in direct methanol PEM fuel cells, were obtained by casting procedures at low and high temperatures.

Water/methanol uptakes of ultra-thin films of the polymers from the vapor phase were measured using a QMB and also from the liquid phase for thick membranes. The partition constant of methanol between the liquid water/methanol mixture and the membranes were determined by immersion of the samples in D_2O followed by ^{1}H NMR determination of the amounts of desorbed H_2O and CH_3OH. The proton conductivities of all the membranes were measured for water saturated membranes at 30 and $60\,^{\circ}$C.

PBI, ABPBI-LT, and ABPBI-HT membranes exhibit lower methanol permeability than Nafion 117 all over the temperature range. A commercial crosslinked ABPBI membrane has lower permeability than the ABPBI-HT membrane, indicating that an optimized casting procedure could be more efficient that crosslinking to reduce methanol crossover in this polymer.

The performance of ABPBI-HT as methanol barrier is somewhat poorer than that of PBI at room temperature, but it is about one order of magnitude less permeable to methanol than Nafion® 117. At higher temperatures the permeation performance of ABPBI-HT is close to that of PBI and it would be even better above $90\,^{\circ}$C. Methanol permeability results are also correlated with differences in water and methanol sorption behavior of these materials. The ratio between the proton conductivity and the methanol permeability coefficient is much higher for the ABPBI-HT membrane as compared to Nafion and PBI. In summary, the combination of low methanol uptake, low methanol permeability and compatible proton conductivity, make ABPBI-HT membranes attractive as electrolyte in DMPEM fuel cells.

Acknowledgments

References

[1] V. Neburchilov, J. Martin, H. Wang, J. Zhang, A review of polymer electrolyte membranes for direct methanol fuel cells, J. Power Sources 169 (2007) 221–238.

[2] Q. Li, J.O. Jensen, R.F. Savinell, N.J. Bjerrum, High temperature proton exchange membrane based on polybenzimidazoles for fuel cells, Prog. Polym. Sci. 34 (2009) 449–477.

[3] J. Asensio, S. Borrós, P. Gómez-Romero, Proton-conducting membranes based on poly(2,5-benzimidazole) (ABPBI) and phosphoric acid prepared by direct acid casting, J. Membr. Sci. 241 (2004) 89–93.

[4] A. Carollo, E. Quartarone, C. Tomasi, P. Mustarelli, F. Belloti, A. Magistris, F. Maestroni, M. Parachini, L. Garlaschelli, P.P. Righetti, Developments of new proton conducting membranes based on different polybenzimidazole structures for fuel cells applications, J. Power Sources 160 (2006) 175–180.

[5] R. He, Q. Li, G. Xiao, N.J. Bjerrum, Proton conductivity of phosphoric acid doped polybenzimidazole and its composites with inorganic proton conductors, J. Membr. Sci. 226 (2003) 169–184.

[6] R. Wycisk, J. Chisholm, J. Lee, J. Lin, P.N. Pintauro, Direct methanol cell membranes from Nafion–polybenzimidazole blends, J. Power Sources 163 (2006) 9–17.

[7] J.A. Ascencio, E.M. Sánchez, P. Gómez-Romero, proton-conducting membranes based on benzimidazole polymers for high-temperature PEM fuel cells. A chemical quest, Chem. Soc. Rev. 39 (2010) 3210–3239.

[8] A. Ainla, D. Brandell, Nafion–polybenzimidazole (PBI) composite membranes for DMFC applications, Solid State Ionics 178 (2007) 581–585.

[9] Q. Li, R. He, J.O. Jensen, N.J. Bjerrum, Approaches and recent development of polymer electrolyte membrane for fuel cells operating above $100\,^{\circ}$C, Chem. Mater. 15 (2003) 4896–4915.

[10] T. Take, K. Tsurutani, M. Umeda, Hydrogen production by methanol–water solution electrolysis, J. Power Sources 164 (2007) 9–16.

[11] Z. Hu, M. Wu, Z. Wei, S. Song, P.K. Shen, Pt–W/C as a cathode electrocatalyst for hydrogen production by methanol electrolysis, J. Power Sources 166 (2007) 458–461.

[12] C.R. Cloutier, D.P. Wilkinson, Electrolytic production of hydrogen from aqueous acidic methanol solutions, Int. J. Hydrogen Energy 35 (2010) 3967–3984.

[13] J.S. Wainright, J.T. Wang, R.F. Savinell, M. Litt, H. Moaddel, C. Rogers, Acid-doped polybenzimidazoles, a new polymer electrolyte, Proc. Electrochem. Soc. 94 (1994) 255–264.

[14] D. Weng, J.S. Wainright, U. Landau, R.F. Savinell, Electro-osmotic drag coefficient of water and methanol in polymer electrolytes at high temperatures, J. Electrochem. Soc. 143 (1996) 1260–1263.

[15] R. He, Q. Li, A. Bach, J.O. Jensen, N.J. Bjerrum, Physicochemical properties of phosphoric acid doped polybenzimidazole membranes for fuel cells, J. Membr. Sci. 277 (2006) 38–45.

[16] S.H. Han, J.E. Lee, K.-J. Lee, H.B. Park, Y.M. Lee, Highly gas permeable and microporous polybenzimidazole membrane by thermal rearrangement, J. Membr. Sci. 357 (2010) 143–151.

[17] S.C. Kumbharkar, U.K. Kharul, Investigation of gas permeation of systematically modified polybenzimidazole by N-substitution, J. Membr. Sci. 357 (2010) 134–142.

[18] S.C. Kumbharkar, U.K. Kharul, New N-substituted ABPBI: synthesis and evaluation of gas permeation properties, J. Membr. Sci. 360 (2010) 418–425.

[19] J.T. Wang, S. Wasmus, R.F. Savinell, Real-time mass spectrometric study of the methanol crossover in a direct methanol fuel cell, J. Electrochem. Soc. 143 (1996) 1233–1239.

[20] H. Pu, Q. Liu, G. Liu, Methanol permeation and proton conductivity of acid-doped poly(N-ethylbenzimidazole) and poly(N-methylbenzimidazole), J. Membr. Sci. 241 (2004) 169–175.

[21] H. Pu, Q. Liu, Methanol permeability and proton conductivity of polybenzimidazole and sulfonated polybenzimidazole, Polym. Int. 53 (2004) 1512–1516.

[22] B.S. Pivovar, Y. Wang, E.L. Cussler, Pervaporation membranes in direct methanol fuel cells, J. Membr. Sci. 154 (1999) 155–162.

[23] J. Lobato, P. Cañizares, M.A. Rodrigo, J.J. Linares, G. Manjavacas, Synthesis and characterisation of poly[2,2-(m-phenylene)-5,5-bibenzimidazole] as polymer electrolyte membrane for high temperature PEMFCs, J. Membr. Sci. 280 (2006) 351–362.

[24] J. Lobato, P. Cañizares, M.A. Rodrigo, J.J. Linares, R. Lopez-Vizcaino, Performance of a vapour-fed polybenzoimidazole (PBI)-based direct methanol fuel cell, Energy Fuels 22 (2008) 3335–3345.

[25] J.S. Wainright, J.-T. Wang, D. Weng, R.F. Savinell, M. Litt, Acid-doped polybenzimidazoles: a new polymer electrolyte, J. Electrochem. Soc. 142 (1995) L121–L123.

[26] L. Gubler, D. Kramer, J. Belack, Ö. Ünsal, T.J. Schmidt, G.G. Scherer, V. Celtec, A polybenzimidazole-based membrane for the direct methanol fuel cell, J. Electrochem. Soc. 154 (2007) B891–B987.

[27] S.-W.S. Chuang, L.-C. Hsu, C.-L. Hsu, Synthesis and properties of fluorine-containing polybenzimidazole/monmorillonite nanocomposite membranes for direct methanol fuel cells applications, J. Power Sources 168 (2007) 172–177.

[28] S.-W.S. Chuang, L.-C. Hsu, Synthesis and properties of a new fluorine-containing polybenzimidazole for high-temperature fuel cell applications, J. Polym. Sci. A: Polym. Chem. 44 (2006) 4508–4512.

[29] L.J. Hobson, Y. Nakano, H. Ozu, S. Hayase, Targeting improved DMFC performance, J. Power Sources 104 (2002) 79–84.

[30] R. Wycisk, J.K. Lee, P.N. Pintauro, Sulfonated polyphosphazene–polybenzimidazole membranes for DMFCs, J. Electrochem. Soc. 152 (2005) A892–A898.

[31] H. Zhang, X. Li, C. Zhao, T. Fu, Y. Shi, H. Na, Composite membranes based on highly sulfonated PEEK and PBI: morphology chararcteristics and performance, J. Membr. Sci. 308 (2008) 66–74.

[32] J.A. Asensio, S. Borrós, P. Gómez-Romero, Proton-conducting polymers based on benzimidazoles and sulfonated benzimidazoles, J. Polym. Sci. A: Polym Chem. 40 (2002) 3703–3710.

[33] L.A. Diaz, G.C. Abuin, H.R. Corti, Water and phosphoric acid uptake of poly[2,5-benzimidazole] (ABPBI) membranes prepared by low and high temperature casting, J. Power Sources 188 (2009) 45–50.

[34] J.A. Asensio, S. Borrós, P. Gómez-Romero, Polymer electrolyte fuel cells based on phosphoric acid-impregnated poly(2,5-benzimidazole) membranes, J. Electrochem. Soc. 151 (2004) A304–A310.

[35] B. Khalfaoui, A. Meniai, R. Borja, Thermodynamic properties of water + normal alcohols and vapor–liquid equilibria for binary systems of methanol or 2-propanol with water, Fluid Phase Equil. 127 (1997) 181–190.

[36] G. Sauerbrey, Verwendung von Schwingquarzen zur Wägung dünner Schichten und zur Mikrowägung, Z. Phys. 155 (1959) 206–222.

[37] Z. Wu, G. Sun, W. Jin, H. Hou, S. Wang, A model for methanol transport through Nafion membrane in diffusion cell, J. Membr. Sci. 325 (2008) 376–382.

[38] L. Chaabane, L. Dammak, D. Grande, C. Larchet, P. Huguet, S.V. Nikonenko, V.V. Nikonenko, Swelling and permeability of Nafion 117 in water–methanol solutions: An experimental and modelling investigation, J. Membr. Sci. 377 (2011) 54–64.

[39] G.C. Abuin, M.C. Fuertes, H.R. Corti, unpublished results.

[40] V. Saarinen, K.D. Kreuer, M. Schuster, R. Merkle, J. Maier, On the swelling properties of proton conducting membranes for direct methanol fuel cells, Solid State Ionics 178 (2007) 533–537.

[41] P. Kauranen, E. Skou, Methanol permeability in perfluorosulfonate proton exchange membranes at elevated temperatures, J. Appl. Electrochem. 26 (1996) 909–917.

[42] V. Tricoli, Proton and methanol transport in poly(perfluorosulfonate) membranes containing Cs$^+$ and H$^+$ cations, J. Electrochem. Soc. 145 (1998) 3798–3801.

[43] V. Tricoli, N. Carretta, M. Bartolozzi, A comparative investigations of proton and methanol transport in fluorinated ionomeric membranes, J. Electrochem. Soc. 147 (2000) 1286–1290.

[44] X. Ren, T. Springer, T. Zawodzinski, S. Gottesfeld, Methanol transport through Nafion membranes. Electro-osmotic drag effects on potential step measurements, J. Electrochem. Soc. 147 (2000) 466–474.

[45] J. Feichtinger, R. Galm, M. Walker, K.-M. Baumgärtner, A. Schulz, E. Räuchle, U. Schumacher, Plasma polymerized barrier films on membranes for direct methanol fuel cells, Surf. Coat. Technol. 142–144 (2001) 181–186.

[46] X. Zhou, J. Weston, E. Chalkova, M. Hofmann, C. Ambler, H. Allcock, S. Lvov, High temperature transport properties of polyphosphazene membranes for direct methanol fuel cells, Electrochim. Acta 48 (2003) 2173–2180.

[47] H.A. Every, M.A. Hickner, J.E. McGrath, J.T.A. Zawodzinski, An NMR study of methanol diffusion in polymer electrolyte fuel cell membranes, J. Membr. Sci. 250 (2005) 183–188.

[48] T. Schaffer, T. Tschinder, V. Hacker, J.O. Besenhard, Determination of methanol diffusion and electrosmotic drag coefficients in proton-exchange-membranes for DMFC, J. Power Sources 153 (2006) 210–216.

[49] S. Xue, G. Yin, Methanol permeability in sulfonated poly(etheretherketone) membranes: a comparison with Nafion membranes, Eur. Polym. J. 42 (2006) 776–785.

[50] Z. Wu, G. Sun, W. Jin, Q. Wang, H. Hou, K.-Y. Chan, Q. Xin, Use of in situ polymerized phenol–formaldehyde resin to modify a Nafion membrane for the direct methanol fuel cell, J. Power Sources 167 (2007) 309–314.

[51] K. Ramya, K.S. Dhathathreyan, Methanol crossover studies of heat-treated Nafion membranes, J. Membr. Sci. 311 (2008) 121–127.

[52] M.P. Godino, V.M. Barragán, M.A. Izquierdo, J.P.G. Villaluenga, B. Seoane, C. Ruiz-Bauzá, Study of the activation energy for transport of water and methanol through a Nafion membrane, Chem. Eng. J. 152 (2009) 20–25.

[53] R. Jiang, H. Russell Kunz, J.M. Fenton, Composite silica/Nafion membranes prepared by tetraethylorthosilicate sol–gel reaction and solution casting for direct methanol fuel cells, J. Membr. Sci. 272 (2006) 116–124.

[54] B.S. Pivovar, W.H. Smyrl, E.L. Cussler, Electro-osmosis in Nafion 117, polystyrene sulfonic acid and polybenzimidazole, J. Electrochem. Soc. 152 (2005) A53–A60.

[55] S. Ochi, O. Kamishima, J. Mizusaki, J. Kawamura, Investigation of proton diffusion in Nafion 117 membrane by electrical conductivity and NMR, Solid State Ionics 180 (2009) 580–584.

[56] Q. Li, H.A. Hjuler, N.J. Bjerrum, Phosphoric acid doped polybenzimidazole membranes: physicochemical characterization and fuel cell applications, J. Appl. Electrochem. 31 (2001) 773–779.

[57] C. Hasiotis, V. Deimede, C. Kontoyannis, New polymer electrolytes based on blends of sulfonated polysulfones with polybenzimidazole, Electrochim. Acta 46 (2001) 2401–2406.

[58] A.V. Anantaraman, C.L. Gardner, Studies on ion-exchange membranes. Part 1. Effect of humidity on the conductivity of Nafion, J. Electroanal. Chem. 414 (1996) 115–120.